

Aroylhydrazone derivative as fluorescent sensor for highly selective recognition of Zn²⁺ ions: syntheses, characterization, crystal structures and spectroscopic properties†Xiaohong Peng,^a Xiaoliang Tang,^a Wenwu Qin,^a Wei Dou,^a Yanling Guo,^a Jiangrong Zheng,^a Weisheng Liu^{*a} and Daqi Wang^b

Received 16th November 2010, Accepted 10th March 2011

DOI: 10.1039/c0dt01590c

A new Zn²⁺ fluorescent chemosensor *N'*-(3,5-di-*tert*-butylsalicylidene)-2-hydroxybenzoylhydrazine (**H₃L¹**) and its complexes [Zn(**HL¹**)C₂H₅OH]_∞ (**1**) and [Cu(**HL¹**)(H₂O)]CH₃OH (**2**) have been synthesized and characterized in terms of their crystal structures, absorption and emission spectra. **H₃L¹** displays high selectivity for Zn²⁺ over Na⁺, K⁺, Mg²⁺, Ca²⁺ and other transition metal ions in Tris–HCl buffer solution (pH = 7.13, EtOH–H₂O = 8 : 2 v/v). To obtain insight into the relation between the structure and selectivity, a similar ligand 3,5-di-*tert*-butylsalicylidene benzoylhydrazine (**H₂L²**), which lacks the hydroxyl group substituent in salicyloyl hydrazide compared with **H₃L¹**, and its complex [Zn₂(**HL²**)₂(CH₃COO)₂(C₂H₅OH)] (**3**), [Co(**L²**)] [Co(DMF)₄(C₂H₅OH)(H₂O)] (**4**), [Fe(**HL²**)₂]Cl·2CH₃OH (**5**), have also been investigated as a reference. **H₃L¹** exhibits improved selectivity for Zn²⁺ compared to **H₂L²**. The findings indicate that the hydroxyl group substituent exerts an effect on the spectroscopic properties, complex structures and selectivity of the fluorescent sensor.

Introduction

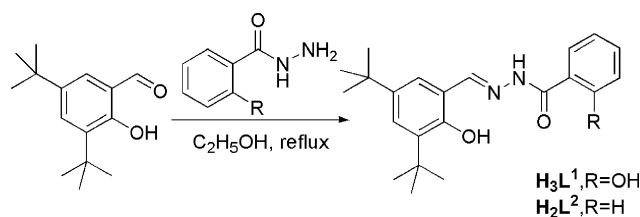
Zn²⁺ ion is an essential nutrient required for normal growth and development¹ and for key cellular processes such as DNA repair² and apoptosis.³ Zn²⁺ deficiency causes unbalanced metabolism, which in turn can induce retarded growth in children, brain disorders, and high blood cholesterol, *etc.*⁴ In this respect, of crucial importance is the design and development of efficient complexing agents that may be used as selective extractants of Zn²⁺ ion and sensors for its detection in solution. There are two challenges in making an effective fluorescent probe for Zn²⁺ detection.⁵ One is to create a probe that responds selectively to Zn²⁺ over other metal ions such as Ca²⁺, Mg²⁺ and Cd²⁺, which compete with Zn²⁺ for the binding sites. The other one is the selectivity of such probes in neutral aqueous solution. In this sense, numerous zinc sensors based on quinoline, fluorescein, coumarin, peptide, and proteins have been designed and reported.^{6,7} Moreover, Schiff bases play a very important role in chemistry as chemosensors being that

the nitrogen exhibits a strong affinity for metal ions, which have been widely used in recognition.^{8–12} Schiff base fluorescent sensors attract special attention owing to their easy synthesis, variable structures and cheap raw materials. So the design and synthesis of simple Schiff-bases as Zn²⁺ sensors for detection in neutral aqueous solution have still attracted considerable attention.

To develop a simple, facile Zn²⁺ fluorescent chemosensor, *N'*-(3,5-di-*tert*-butylsalicylidene)-2-hydroxybenzoylhydrazine (**H₃L¹**) (Scheme 1) was synthesized and characterized. The absorption and fluorescence properties of **H₃L¹** in Tris–HCl buffer solution (pH = 7.13, EtOH–H₂O = 8 : 2 v/v) were investigated. The complexes [Zn(**HL¹**)C₂H₅OH]_∞ (**1**) and [Cu(**HL¹**)(H₂O)]CH₃OH (**2**) were characterized by elemental analysis and single-crystal X-ray structural determination. Moreover, 3,5-di-*tert*-butylsalicylidene benzoylhydrazine (**H₂L²**) (Scheme 1) and its complex [Zn₂(**HL²**)₂(CH₃COO)₂(C₂H₅OH)] (**3**), [Co(**L²**)] [Co(DMF)₄(C₂H₅OH)(H₂O)] (**4**), [Fe(**HL²**)₂]Cl·2CH₃OH (**5**) were also investigated as a reference. The selectivity

^aKey Laboratory of Nonferrous Metal Chemistry and Resources Utilization of Gansu Province and State Key Laboratory of Applied Organic Chemistry, College of Chemistry and Chemical Engineering, Lanzhou University, Lanzhou, 730000, P. R. China. E-mail: liuw@s@lzu.edu.cn; Fax: +86-931-8912582; Tel: +86-931-8915151

^bDepartment of Chemistry, Liaocheng University, Liaocheng, 252000, China † Electronic supplementary information (ESI) available: Crystallographic details in CIF format for **1–5**, tables of interatomic distances and angles for **1–5**, additional spectra for **H₃L¹** and **H₂L²**, and ¹H and ¹³C NMR data. CCDC reference numbers 727397, 727400, 727396, 727399, and 727401. For ESI and crystallographic data in CIF or other electronic format see DOI: 10.1039/c0dt01590c



Scheme 1 Schematic illustration of preparation of ligands **H₃L¹** and **H₂L²**.

of H_3L^1 and H_2L^2 to Zn^{2+} ion, the effects of the hydroxyl group substituent in salicyloyl hydrazide on fluorescent intensity both in solution and solid-state, and the complex structures were investigated in detail.

Experimental

The commercially available chemicals were used without further purification. All of the solvents used were of analytical reagent grade. C, N and H were determined using an Elementar Vario EL. Melting points were determined on a Kofler apparatus. IR spectra were recorded on Nicolet FT-170SX instrument using KBr discs in the 400–4000 cm^{-1} region. ^1H NMR and ^{13}C NMR spectra were measured on a Bruker DRX 400 spectrometer in DMSO-d_6 or CD_3OD solution with TMS as internal standard. Chemical shift multiplicities are reported as s = singlet, t = triplet, q = quartet and m = multiplet. Mass spectra were recorded on a Bruker Daltonics esquire6000 Mass spectrometer. UV absorption spectra were recorded on a Varian Cary 100 spectrophotometer using quartz cells of 1.0 cm path length. Fluorescence measurements were made on a Hitachi F-4500 spectrophotometer and a shimadzu RF-540 spectrofluorophotometer equipped with quartz cuvettes of 1 cm path length with a xenon lamp as the excitation source. An excitation and emission slit of 2.5 nm were used for the measurements in the solution state.

Preparation of ligands and their complexes

***N'*-(3,5-Di-*tert*-butylsalicylidene)-2-hydroxybenzoyl hydrazine (H_3L^1).** To a stirred solution of 3,5-di-*tert*-butyl-2-hydroxybenzaldehyde (1.17 g, 5 mmol) in ethanol was added salicyloyl hydrazide (0.76 g, 5 mmol). The reaction mixture was refluxed for 8 h and then cooled to room temperature. Yellow precipitates formed were filtered and washed with ethanol and dried under vacuum. Yield: (1.472 g) 80%. Mp: 230–232 °C. ESI-MS: m/z 369.1 ($\text{M} + \text{H}^+$). FT-IR (KBr phase) (cm^{-1}): 3437 w, 3238 w, 2956 vs, 1641 vs, 1609 vs, 1556 m, 1489 w, 1360 s, 1306 s, 1233 s, 1174 m, 752 m, 669 w, 531 w. ^1H NMR (400 MHz, CD_3OD , ppm): δ 1.24 (9H, s, $-\text{CH}_3$), 1.38 (9H, s, $-\text{CH}_3$), 6.88–6.90 (2H, m, Ar–H), 7.10 (1H, s, Ar–H), 7.33–7.35 (2H, m, Ar–H), 7.8 (1H, s, Ar–H), 8.40 (1H, s, $\text{CH}=\text{N}$). ^{13}C NMR (400 MHz, CD_3OD , ppm): δ 29.99, 31.90, 35.05, 36.04, 116.35, 118.33, 118.45, 120.51, 127.15, 127.71, 129.57, 135.37, 137.68, 142.22, 154.04, 156.61, 160.80, 166.55.

3,5-Di-*tert*-butylsalicylidene benzoylhydrazine (H_2L^2). To a stirred solution of 3,5-di-*tert*-butyl-2-hydroxybenzaldehyde (1.17 g, 5 mmol) in ethanol was added benzhydrazide (0.68 g, 5 mmol). The reaction mixture was refluxed for 8 h and then cooled to room temperature. White precipitates formed were filtered and washed with ethanol and dried under vacuum. Yield: (1.30 g) 73.9%. Mp: 258.8–259.4 °C. ESI-MS: m/z 353.2 ($\text{M} + \text{H}^+$). FT-IR (KBr phase) (cm^{-1}): 3187 w, 3030 m, 2956 vs, 1645 vs, 1645 vs, 1611 s, 1566 s, 1435 s, 1361 s, 1287 s, 1252 m, 1088 m, 958 w, 890 w, 692 s, 533 w. ^1H NMR (400 MHz, DMSO-d_6 , ppm): δ 1.28 (9H, s, $-\text{CH}_3$), 1.40 (9H, s, $-\text{CH}_3$), 7.20–7.94 (7H, m, Ar–H), 8.57 (1H, s, $\text{CH}=\text{N}$). ^{13}C NMR (400 MHz, DMSO-d_6 , ppm): δ 29.26, 31.26, 33.85, 34.62, 116.94, 125.55, 125.71, 127.61, 128.57, 132.04, 132.61, 135.63, 140.39, 151.27, 154.69, 162.77.

Synthesis of $[\text{Zn}(\text{HL}^1)\text{C}_2\text{H}_5\text{OH}]_\infty$ (1). An ethanol solution of $\text{Zn}(\text{CH}_3\text{COO})_2 \cdot 2\text{H}_2\text{O}$ (0.0109 g, 0.05 mmol) was added slowly to a magnetically stirred 5 mL ethanol solution of the ligand (H_3L^1) (0.0184 g, 0.05 mmol). The mixture was stirred in air for 2 h whereby a yellow solution was formed. It was filtered and kept in air. Yellow block single crystals of **1** suitable for X-ray crystallography were obtained on slow evaporation of the filtrate at ambient temperature within 5 days (yield: 0.0187 g, 63.8%). Anal. Calcd for $\text{C}_{52}\text{H}_{76}\text{N}_4\text{O}_{10}\text{Zn}_2$: C, 59.07; H, 6.076; N, 5.527. Found: C, 59.66; H, 7.27; N, 5.35. FT-IR (KBr phase) (cm^{-1}): 3423 w, 3199 w, 2956 s, 1611 vs, 1561 vs, 1388 m, 1254 w, 1167 m, 691 m, 474 w.

Synthesis of $[\text{Cu}(\text{HL}^1)(\text{H}_2\text{O})] \cdot \text{CH}_3\text{OH}$ (2). A methanol solution $\text{Cu}(\text{CH}_3\text{COO})_2 \cdot \text{H}_2\text{O}$ (0.0100 g, 0.05 mmol) was added slowly to a magnetically stirred 5 mL methanol solution of the ligand (H_2L^2) (0.0176 g, 0.05 mmol). The mixture was stirred in air for 2 h whereby a dark green solution was formed. It was filtered and kept in air. Dark green single crystals of **2** suitable for X-ray crystallography were obtained on slow evaporation of the filtrate at ambient temperature within 5 days. (yield: 0.0130 g, 47.1%). Anal. Calcd for $\text{C}_{23}\text{H}_{32}\text{CuN}_2\text{O}_5$: C, 57.50; H, 6.67; N, 5.83. Found: C, 57.61; H, 6.30; N, 5.48. FT-IR (KBr phase) (cm^{-1}): 3370 w, 3212 w, 2955 vs, 1614 vs, 1524 vs, 1490 s, 1360 s, 1252 s, 1169 s, 752 m, 696 w, 494 w.

Synthesis of $[\text{Zn}_2(\text{HL}^2)_2(\text{CH}_3\text{COO})_2(\text{C}_2\text{H}_5\text{OH})]$ (3). An ethanol solution of $\text{Zn}(\text{CH}_3\text{COO})_2 \cdot 2\text{H}_2\text{O}$ (0.0109 g, 0.05 mmol) was added slowly to a magnetically stirred 5 mL ethanol solution of the ligand (H_2L^2) (0.0176 g, 0.05 mmol). The mixture was stirred in air for 2 h whereby a yellow solution was formed. It was filtered and kept in air. Yellow block single crystals of **3** suitable for X-ray crystallography were obtained on slow evaporation of the filtrate at ambient temperature within 5 days (yield: 0.0158 g, 55.4%). Anal. Calcd for $\text{C}_{50}\text{H}_{66}\text{N}_4\text{O}_9\text{Zn}_2$: C, 60.11; H, 6.34; N, 5.88. Found: C, 60.24; H, 6.63; N, 5.62. FT-IR (KBr phase) (cm^{-1}): 3424 w, 2958 s, 2869 w, 1592 s, 1521 vs, 1434 s, 1386 s, 1248 m, 1165 m, 712 m, 519 w.

Synthesis of $[\text{Co}_2(\text{L}^2)_2(\text{DMF})_2(\text{C}_2\text{H}_5\text{OH})(\text{H}_2\text{O})]$ (4). An ethanol solution of $\text{Co}(\text{CH}_3\text{COO})_2 \cdot 4\text{H}_2\text{O}$ (0.0125 g, 0.05 mmol) was added slowly to a magnetically stirred 5 mL ethanol solution of the ligand (H_2L^2) (0.0176 g, 0.05 mmol). The mixture was stirred in air for 30 min whereby a brown precipitate was formed. Then adding DMF till the precipitate was completely dissolved. It was filtered and kept in air. Black block single crystals suitable for X-ray crystallography were obtained on slow evaporation of the filtrate at ambient temperature within 7 days (yield: 0.0155 g, 51.5%). Anal. Calcd for $\text{C}_{102}\text{H}_{140}\text{Co}_2\text{N}_{12}\text{O}_{14}$: C, 63.59; H, 7.12; N, 8.54. Found: C, 63.26; H, 7.24; N, 8.68. FT-IR (KBr phase) (cm^{-1}): 3422 m, 2927 w, 2361 vs, 2338 s, 1655 m, 1544 w, 1386 m, 1114 m, 669 m, 486 w.

Synthesis of $[\text{Fe}(\text{HL}^2)_2]\text{Cl} \cdot 2\text{CH}_3\text{OH}$ (5). A methanol solution of $\text{FeCl}_3 \cdot 6\text{H}_2\text{O}$ (0.0135 g, 0.05 mmol) was added slowly to a magnetically stirred 5 mL methanol solution of the ligand (H_2L^2) (0.0176 g, 0.05 mmol). The mixture was stirred in air for 30 min whereby a black solution was formed. It was filtered and kept in air. Black block single crystals of **5** suitable for X-ray crystallography were obtained on slow evaporation of the filtrate at ambient temperature within 7 days (yield: 0.0154 g, 49.5%). Anal. Calcd

Table 1 Crystal data for 1–5

Compound reference	1	2	3	4	5
Chemical formula	C ₅₂ H ₇₆ N ₄ O ₁₀ Zn ₂	C ₂₃ H ₃₂ CuN ₂ O ₅	C ₅₀ H ₆₆ N ₄ O ₉ Zn ₂	C ₁₀₂ H ₁₄₀ Co ₃ N ₁₂ O ₁₄	C ₄₆ H ₆₂ ClFeN ₄ O ₆
Formula Mass	1047.9	480.05	997.81	1935.05	858.30
Crystal system	Triclinic	Triclinic	Monoclinic	Tetragonal	Triclinic
<i>a</i> /Å	7.7586(6)	6.8520(8)	16.739(2)	16.175(2)	11.801(11)
<i>b</i> /Å	11.1224(15)	9.5110(10)	10.4668(11)	16.175(2)	13.610(12)
<i>c</i> /Å	17.327(2)	19.477(2)	29.254(3)	41.560(3)	14.805(13)
α (°)	96.667(2)	99.223(2)	90.00	90.00	88.618(13)
β (°)	102.141(3)	93.968(2)	99.362(2)	90.00	86.079(12)
γ (°)	95.722(2)	105.547(3)	90.00	90.00	88.823(12)
Unit cell volume/Å ³	1440.0(3)	1198.6(2)	5057.1(10)	10873(2)	2371(4)
<i>T</i> /K	293(2)	298(2)	298(2)	298(2)	298(2)
Space group	<i>P</i> 1	\bar{P} 1	<i>P</i> 2 ₁ / <i>c</i>	<i>p</i> 43212	\bar{P} 1
No. of formula units per unit cell, <i>Z</i>	1	2	4	4	2
No. of reflections measured	7433	6246	25503	54507	12409
No. of independent reflections	6034	4134	8913	9576	8212
<i>R</i> _{int}	0.0438	0.0254	0.0517	0.1518	0.0339
Final <i>R</i> ₁ values (<i>I</i> > 2σ(<i>I</i>))	0.0762	0.0596	0.0458	0.0785	0.0483
Final <i>wR</i> (<i>F</i> ²) values (<i>I</i> > 2σ(<i>I</i>))	0.1732	0.1450	0.1024	0.1913	0.0914
Final <i>R</i> ₁ values (all data)	0.1339	0.0827	0.0844	0.1197	0.0959
Flack parameters	0.01 (3)			0.02 (3)	
Final <i>wR</i> (<i>F</i> ²) values (all data)	0.2072	0.1606	0.1214	0.2132	0.1035

for C₄₆H₆₂ClFeN₄O₆: C, 64.37; H, 7.23; N, 6.53. Found: C, 64.26; H, 7.24; N, 6.68. FT-IR (KBr phase) (cm⁻¹): 3431 s, 2957 s, 1606 vs, 1546 vs, 1414 w, 1384 m, 1250 w, 1177 m, 706 m, 679 w, 543 m, 467 w (w, weak; m, medium; s, strong; vs, very strong).

X-ray crystallography

The X-ray diffraction data were collected on a Bruker SMART 1000 CCD diffractometer operating at 50 KV and 30 mA using graphite-monochromated Mo-K α radiation source (λ = 0.71073 Å). An empirical absorption correction based on the comparison of redundant and equivalent reflections was applied using SADABS. A summary of crystallographic data and details of the structure refinements are listed in Table 1. The structure was solved by direct methods and refined by full matrix least-squares techniques on *F*² with all non-hydrogen atoms treated anisotropically. All calculations were performed with the program package SHELXTL. The hydrogen atoms were assigned with common isotropic displacement factors and included in the final refinement by using geometrical restraints. The structural data have been deposited with the Cambridge Crystallographic Data Centre (CCDC) with reference numbers 727397, 727400, 727396, 727399, and 727401 for compounds 1–5, respectively.

Results and discussion

X-ray diffraction studies

Crystal structure of [Zn(HL¹)C₂H₅OH]_n (1). As shown in Fig. 1b, the crystal is a 1-D zigzag coordination polymer. The asymmetric unit contains two crystallographically independent Zn²⁺ ions (Zn1 and Zn2). Each Zn²⁺ center is coordinated to a chelating H₃L¹ ligand, an ethanol molecule and the O donor of a neighboring [Zn(HL¹)C₂H₅OH] unit. The geometry around the Zn²⁺ center (Zn1) can be described as a distorted square pyramid where the oxygen atom of the ethanol molecule (O7) occupies the apical position, the atoms O2, O6, N4, O4 define the basal plane, and the metal atom is placed at 0.512 Å (Zn1) from the basal plane.

Zn2 is similar to Zn1, while Zn atom is placed at 0.490 Å (Zn2) from the basal planes. The bond lengths of Zn–phenoxo (Zn1–O2 = 1.924(9) Å; Zn1–O6 = 1.965(8) Å; Zn2–O5 = 1.945(9) Å; Zn2–O3 = 1.955(9) Å) are much shorter than that of Zn–N (Zn1–N4 = 2.054(11) Å; Zn2–N2 = 2.067(12) Å), which shows that the strength of Zn–O bonds are stronger than Zn–N bonds, while Zn–O carbonyl oxygen bonds are weaker than Zn–N bonds (Zn1–O4 = 2.197(10) Å; Zn2–O1 = 2.249(11) Å). The aroylhydrazone remained in the keto form. Each of these chains is linked by extensive O–H...O hydrogen bonds involving the H atoms in L¹ and O atoms in ethanol molecule into a 3D coordination network. (Fig. 1c) Two 1D chains are further connected to a 1D double chain coordination supramolecule by hydrogen bonds. The zigzag chains are aligned one above the other and are held together in a three-dimensional hydrogen-bonded network by interactions between the ethanol.

Crystal structure of [Cu(HL¹)(H₂O)]·CH₃OH (2). As shown in Fig. 2, the phenoxo are not coordinated with copper. Copper is four coordinate using a tridentate Schiff base ligand, and a water molecule. The copper center adopts distorted square planar coordination geometry.

Crystal structure of [Zn₂(HL²)₂(CH₃COO)₂(C₂H₅OH)] (3). As shown in Fig. 3, a unit contains a Zn dinuclear cation, one acetic anion, and an ethanol solvent molecule, which is obviously different from complex 1. The geometry of each Zn²⁺ ion is best described as square-pyramidal with varying amount of trigonal bipyramidal distortion across the mononuclear units, where one of the Zn²⁺ (Zn1) is coordinated by O₂N of the H₂L² unit, a oxygen atom of the acetate; while the other Zn²⁺ (Zn2) is coordinated by the H₂L² unit and ethanol. These two Zn²⁺ centers are bridged by the two oxygen atoms of an acetic ion, with the bond distances: Zn2–O4 = 1.980(3) Å, Zn1–O3 = 2.020(2) Å; and Zn...Zn separation about 6.0406 Å. There are two acetic anions in the crystal structure. One acts as a bridge while the other one is only coordinated with Zn²⁺.

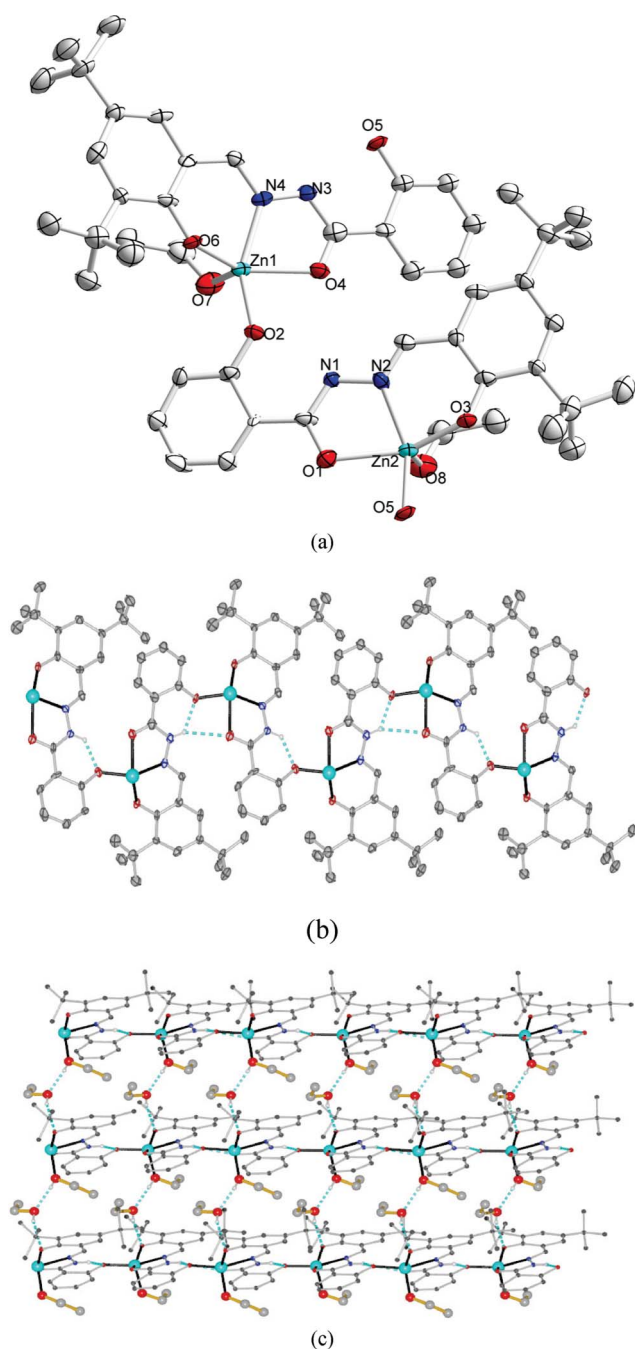


Fig. 1 (a) Molecular structure of $[\text{Zn}_2(\text{HL}^1)_2(\text{C}_2\text{H}_5\text{OH})_2]$ (**1**) showing the local coordination geometry along with atom labeling schemes and 30% thermal ellipsoids. (b) Portion of the infinite zigzag chain. Hydrogen atoms and crystal lattice solvent molecules are omitted for clarity. (c) 3D stacking structure of complex **1**. Hydrogen bonds are shown as dashed lines.

Crystal structure of $[\text{Co}(\text{L}^2)_2][\text{Co}(\text{DMF})_4(\text{C}_2\text{H}_5\text{OH})(\text{H}_2\text{O})]$ (4**).** The crystal structure of **4** contains two crystallographically independent species: one complex cation $[\text{Co}(\text{DMF})_4(\text{C}_2\text{H}_5\text{OH})(\text{H}_2\text{O})]^{2+}$ and one complex anion $[\text{Co}(\text{L}^2)_2]^{2-}$. As shown in Fig. 4, $\text{Co}2$ is absolutely coordinated by solvent molecules such as DMF, water and ethanol in a perfectly octahedral geometry (being angles: $\text{O}8-\text{Co}2-\text{O}7 = 180.00^\circ$, $\text{O}5-\text{Co}2-\text{O}6 = 90.9^\circ$; $\text{O}5-\text{Co}2-\text{O}6 = 89.1^\circ$). The geometry at the

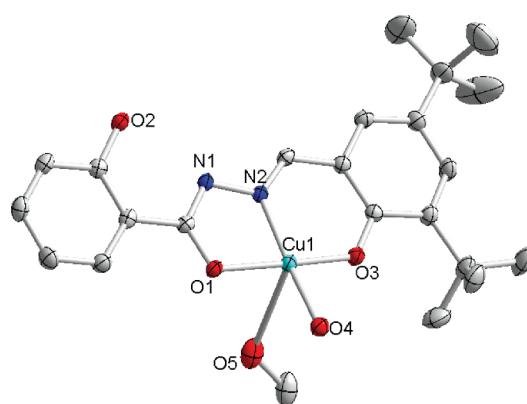


Fig. 2 Structure of $[\text{Cu}(\text{HL}^1)(\text{H}_2\text{O})] \cdot \text{CH}_3\text{OH}$ showing the coordination sphere of Cu^{2+} in complex **2** along with atom labeling schemes and 30% thermal ellipsoids. Hydrogen atoms and crystal lattice solvent molecules are omitted for clarity.

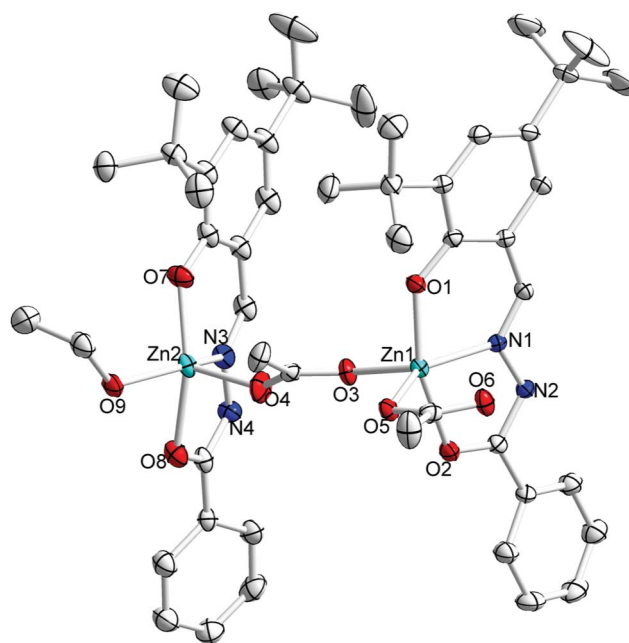


Fig. 3 Structure of $[\text{Zn}_2(\text{HL}^2)_2(\text{CH}_3\text{COO})_2(\text{C}_2\text{H}_5\text{OH})]$ showing the coordination sphere of Zn^{2+} in complex **3** along with atom labeling schemes and 30% thermal ellipsoids. Hydrogen atoms and crystal lattice solvent molecules are omitted for clarity.

$\text{Co}1$ is best described as distorted octahedral. Co^{2+} center is six coordinate using two tridentate Schiff base ligands.

Crystal structure of $[\text{Fe}(\text{HL}^2)_2]\text{Cl} \cdot 2\text{CH}_3\text{OH}$ (5**).** The geometry of the Fe^{3+} center in compound **5** is best described as a distorted octahedral, comprising two equivalent tridentate ligands (Fig. 5). Each of the two equivalent aroylhydrazone ligands coordinates to the Fe^{3+} ion with the phenolate oxygen (O3), imine nitrogen (N3), and keto oxygen (O4) donor atoms to form a pseudooctahedral geometry.¹³

Fluorescence spectra and titration

The emission spectrum of the sensor H_2L^1 ($\Phi = 0.00132$) excited at 336 nm exhibits the emission maximum at 505 nm in Tris-HCl buffer solution ($\text{pH} = 7.13$, $\text{EtOH-H}_2\text{O} = 8:2 \text{ v/v}$) at

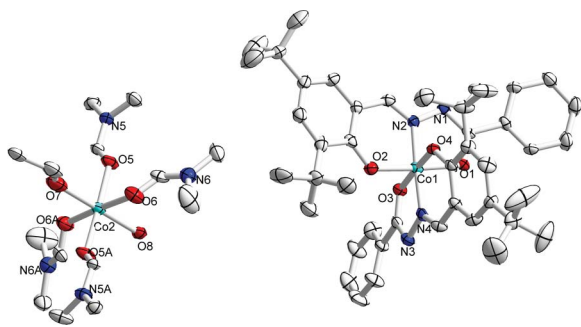


Fig. 4 Structure of $[\text{Co}(\text{L}^2)_2][\text{Co}(\text{DMF})_4(\text{C}_2\text{H}_5\text{OH})(\text{H}_2\text{O})]$ (**4**) showing the coordination sphere of Co^{2+} in complex **4** along with atom labeling schemes and 30% thermal ellipsoids. Hydrogen atoms are omitted for clarity. Symmetry code: (A) $y, x, -z$.

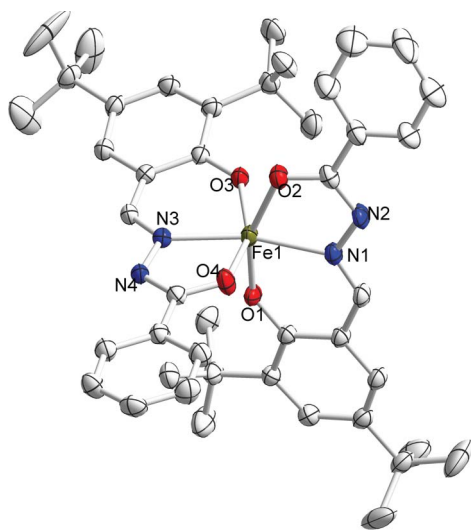


Fig. 5 Structure of $[\text{Fe}(\text{HL}^2)]^+$ showing the coordination sphere of Fe^{3+} in complex **5** along with atom labeling schemes and 30% thermal ellipsoids. Hydrogen atoms and crystal lattice solvent molecules are omitted for clarity.

25 °C. We measured the emission intensities of the sensor molecule in the presence of various concentrations of Zn^{2+} (0–0.1 mM concentration).

Job's plot analysis (Fig. S5†) revealed maximum emission at 1 : 1 ratio ($\text{H}_3\text{L}^1 : \text{Zn}^{2+}$), which is in good agreement with the absorption study results and the X-ray structure of the zinc complex. This result has also been confirmed by ESI-MS, where a peak at m/z 477.3 corresponding to the 1 : 1 complex $[\text{HL}^1 \cdot \text{Zn}^{2+} \cdot \text{C}_2\text{H}_5\text{OH}]^+$ is observed. To observe the binding interaction with Zn^{2+} , the binding constant value has been determined from the emission intensity data following the modified Benesi–Hildebrand equation:¹⁴ $1/\Delta F = 1/\Delta F_{\text{max}} + (1/K[\text{C}])(1/\Delta F_{\text{max}})$. Here $\Delta F = F_x - F_0$ and $\Delta F_{\text{max}} = F_{\infty} - F_0$, where F_0 , F_x , and F_{∞} are the emission intensities of H_3L^1 considered in the absence of Zn^{2+} , at an intermediate Zn^{2+} concentration, and at a concentration of complete interaction, respectively, and where K is the binding constant and $[\text{C}]$ the Zn^{2+} concentration. From the plot of $(F_{\infty} - F_0)/(F_x - F_0)$ against $[\text{C}]^{-1}$ for H_3L^1 , the value of K extracted from the slope is $2.9792 \times 10^5 \text{ M}^{-1}$.

Upon the addition of 10 equivalents of Zn^{2+} , the fluorescence intensity of H_3L^1 increases by 25-fold, and the quantum yield

is 0.03236. The experiment reveals that there is a significant increase in fluorescence intensity for **1**, the emission from $[\text{Zn}(\text{HL}^1)\text{C}_2\text{H}_5\text{OH}]_{\infty}$ (**1**) is believed to arise from an excited-state centered on H_3L^1 which contains two phenolic protons, which will deprotonate upon complexation with Zn^{2+} .

As illustrated in Fig. 6(b), among the metal ions studied, only Zn^{2+} significantly changes the fluorescence spectra of H_3L^1 . Other cations which exist at high concentration in living cells, such as Na^+ , K^+ , Mg^{2+} , and Ca^{2+} did not change the Zn^{2+} -induced emission, even when present in large excess. Paramagnetic ions, such as Cu^{2+} , Cr^{3+} , Fe^{3+} quench the emission, owing to an electron or energy transfer between the metal cation and fluorophore known as the fluorescence quenching mechanism.¹⁵ Almost no influence of the first-row transition-metal ions such as Mn^{2+} , Co^{2+} , and Ni^{2+} (100 μM) on the fluorescence intensity of H_3L^1 was observed. The presence of heavy metal ions including Cd^{2+} , a d^{10} ion that often exhibits coordination properties similar to Zn^{2+} (50 μM), do not interfere with the emission of the Zn^{2+} - HL^1 complex (Fig. S6†). The high selectivity of H_3L^1 for Zn^{2+} over other metal ions should be in part attributed to the strong coordination

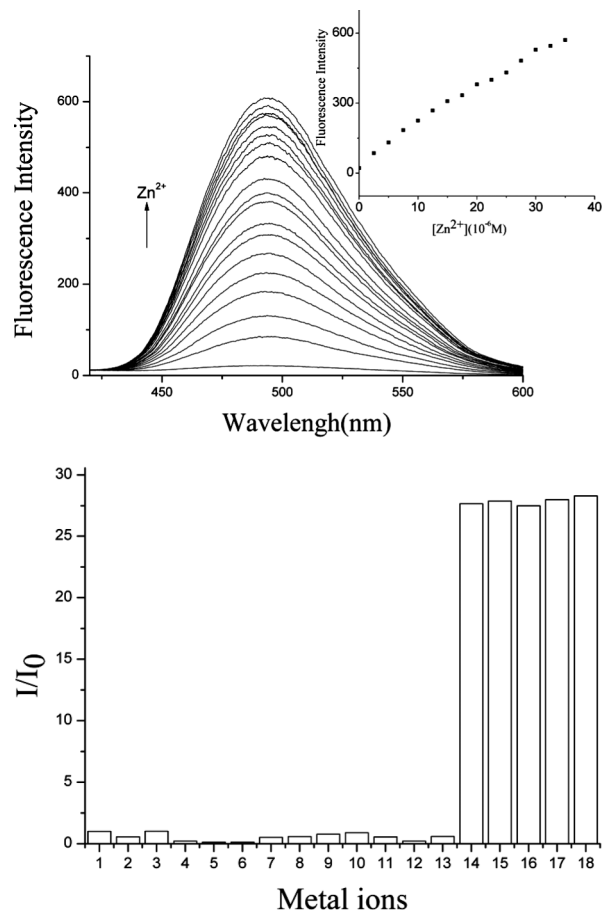


Fig. 6 (a) Increasing concentrations of Zn^{2+} (0, 1.0, 2.5, 5.0, 7.5, 10, 15, 20, 25, 30, 35, 40, 45, 50 μM). Inset: fluorescence intensity of H_3L^1 at 505 nm vs. equiv of Zn^{2+} . (b) Fluorescent emission changes of H_3L^1 ($1.0 \times 10^{-5} \text{ mol L}^{-1}$) upon addition of 1, blank; 2, Ag^+ ; 3, Cd^{2+} ; 4, Co^{2+} ; 5, Cr^{3+} ; 6, Cu^{2+} ; 7, Fe^{3+} ; 8, Hg^{2+} ; 9, Li^+ ; 10, Mg^{2+} ; 11, Mn^{2+} ; 12, Ni^{2+} ; 13, Ca^{2+} ; 14, Zn^{2+} ; 15, $\text{Zn}^{2+} + \text{Li}^+$; 16, $\text{Zn}^{2+} + \text{Na}^+$; 17, $\text{Zn}^{2+} + \text{Mg}^{2+}$; 18, $\text{Zn}^{2+} + \text{Ca}^{2+}$ (10 equiv) in Tris–HCl buffer solution (pH = 7.13, EtOH– H_2O = 8 : 2 v/v) at room temperature. Excitation wavelength was 336 nm.

ability of Zn^{2+} . To understand the fluorescence enhancement and quench of H_3L^1 when binding Zn^{2+} and Cu^{2+} , respectively, we can compare the crystal structures of the two complexes. The d^{10} ion has distinct properties such as Zn^{2+} , Zn^{2+} coordinated with aroylhydrazone extends the rigidity of the ligand. Meanwhile, as shown in Fig. 1 and 2, crystals **1** and **2** could act as references for the coordination mode of Zn^{2+} and Cu^{2+} with H_3L^1 .

Effect of pH

In addition to metal ion selectivity, we measured the fluorescence intensity of H_3L^1 at various pH values in the presence and absence of Zn^{2+} . As can be seen from Fig. 7, the emission intensity of H_3L^1 decreases under acidic conditions. And essentially no change can be observed under neutral and alkaline conditions (pH 7–12). Interestingly, H_3L^1 showed good fluorescence sensing ability to Zn^{2+} over a wide range of pH values. This property arises from protonation of the phenolic hydroxyl group of the ligand. H_3L^1 shows no appreciable sensing ability to Zn^{2+} at a pH below 6.1, which may be due to the competition of H^+ below pH 6.1, but exhibits satisfactory Zn^{2+} sensing abilities when the pH is increased to the range 6.3–10, which is suitable for measurements.

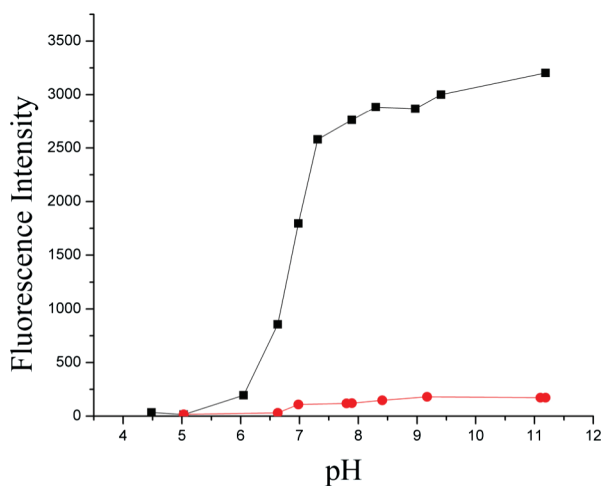


Fig. 7 Fluorescence intensities of H_3L^1 and Zn^{2+} at various pH values at room temperature, Tris–HCl buffer solution (pH = 7.13, EtOH– H_2O = 8 : 2 v/v), λ_{exc} = 336 nm; black line, the fluorescence intensities at 565 nm of Zn^{2+} – HL^1 at various pH ($[\text{H}_3\text{L}^1]$ = 10 μM [Zn^{2+}] = 0.10 mM); Red line, the fluorescence intensities at 515 nm of H_3L^1 at various pH ($[\text{H}_3\text{L}^1]$ = 10 μM , [Zn^{2+}] = 100 μM).

The fluorescence enhancement effects of various metal ions on H_2L^2 were investigated under excitation at 316 nm (Fig. 8). In the absence of metal ions, H_2L^2 exhibited a very weak fluorescence peak near 485 nm. When Zn^{2+} was introduced to a 10 μM solution of H_2L^2 in ethanol, obvious red shift (~38 nm) and enhancement of fluorescence spectra were observed, whereas other ions of interest displayed much weaker response. Upon addition of 5 equivalents of Zn^{2+} , ligand H_2L^2 displayed only 5.27-fold increase in fluorescence intensity. The fluorescence intensity had little change when addition of more Zn^{2+} . The quantum yield of H_2L^2 is 0.00297. The value changes to 0.01728 after the addition of Zn^{2+} ion in the H_2L^2 solution. The H_2L^2 and Zn^{2+} form complex of 1 : 2 stoichiometry, which could be confirmed by ESI-MS spectrum (m/z 767.5) and crystal structure. Moreover,

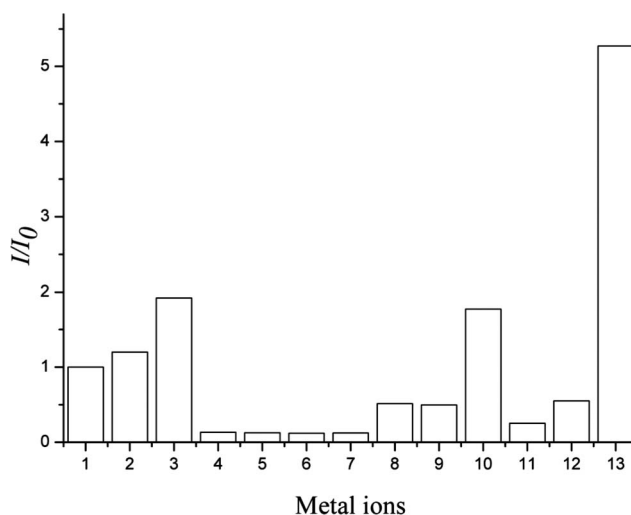


Fig. 8 Fluorescent emission changes of H_2L^2 (1.0×10^{-5} mol L^{-1}) upon addition of 1, blank; 2, Ag^+ ; 3, Cd^{2+} ; 4, Co^{2+} ; 5, Cr^{3+} ; 6, Cu^{2+} ; 7, Fe^{3+} ; 8, Hg^{2+} ; 9, Li^+ ; 10, Mg^{2+} ; 11, Mn^{2+} ; 12, Ni^{2+} ; 13, Zn^{2+} (5 eq.) in ethanol. Excitation wavelength was 316 nm.

Co^{2+} and Fe^{3+} quenched the fluorescence intensity of the H_2L^2 . To better understand the interaction of H_2L^2 and metal ions, we also obtained the crystal structure of these two metal ions. The crystal structure and ESI-MS spectrum (m/z 758.5 and 761.5) show that the metals and H_2L^2 also form complexes of 1 : 2 stoichiometry.

Water quenched the fluorescence intensity of the Zn^{2+} – H_2L^2 system, and the fluorescence intensity of H_2L^2 had a very small increase in aqueous ethanol solution upon the addition of 5 equivalents of Zn^{2+} . The selectivity of the H_2L^2 for Zn^{2+} ion in aqueous ethanol solution is too low to be observed.

The H_3L^1 – Zn complex exhibits 20 times higher emission increase than unsubstituted H_2L^2 – Zn complex, indicating a significant fluorescence enhancement achieved by the introduction of a hydroxyl group.

We also studied the fluorescence intensity in solid-state Zn^{2+} – HL^1 and Zn^{2+} – HL^2 and found that the former is much higher than the latter under the same conditions (see supporting information Fig. S7†). When we compare the Zn^{2+} complexes of the two ligands, we can find that the hydroxyl group in salicyloyl hydrazone gets involved in the coordination environment, which is in accord with the crystal structure of Zn^{2+} – HL^1 and Zn^{2+} – HL^2 .

Absorption study

The absorption spectrum of H_3L^1 (10 μM) exhibits a maximal absorption at 294 nm and 349 nm before titration at room temperature in Tris–HCl buffer solution (pH = 7.13, EtOH– H_2O = 8 : 2 v/v) (Fig. 9). Upon addition of Zn^{2+} (0–2 equiv), the absorbance at 294 nm and 349 nm reduced gradually. Meanwhile, a new absorption peak appeared at 417 nm, which could be attributed to the interaction between the ligand moiety and zinc. The new absorption band (417 nm) of Zn – HL^1 may arise from two effects. First, the phenolic proton of the ligand is deprotonated. The binding of $[\text{HL}^1]^{2-}$ to Zn^{2+} can form a six-membered chelate ring with the Schiff base $\text{C}=\text{N}$ and $\text{Ar}-\text{O}^-$, which enlarges the conjugated system, and thus reduces the energy difference between n and π^* orbital.¹⁶ Second, in the absence of a metal ion, H_3L^1 does

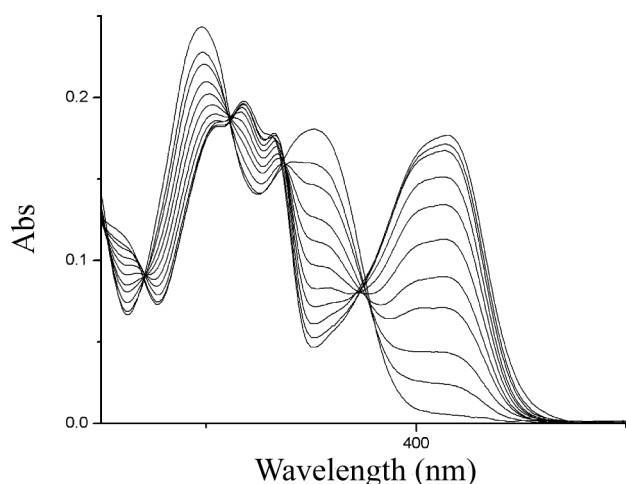


Fig. 9 UV-vis spectra changes of H_3L^1 (10 μM) upon addition of Zn^{2+} in Tris-HCl buffer solution (pH = 7.13, EtOH-H₂O = 8:2 v/v) at room temperature. ($[\text{Zn}^{2+}] = 0, 1, 2, 3, 4, 5, 6, 7, 8, 9, 10 \mu\text{M}$).

not show noticeable emission when excited at 417 nm because the C=N bond *cis*↔*trans* isomerization may be the predominant decay process in the excited state.¹⁷

Moreover, there are isosbestic points at 268 nm and 375 nm, which indicate the presence of only two species in equilibrium. When addition of Mg^{2+} or Cd^{2+} (0–2 equiv), as shown in Fig. S8† the change of absorbance is not obvious.

The UV-vis titration curve of H_2L^2 with added Zn^{2+} in ethanol at 25 °C can be seen in the supporting information (Fig. S9†). The UV-vis spectra of sensors H_3L^1 and H_2L^2 are nearly identical.

Conclusion

In conclusion, we have succeeded in preparing two simple and easy-to-make Zn^{2+} cation chemosensors H_3L^1 and H_2L^2 . Spectroscopic properties and crystal structures with respect to Zn^{2+} coordination of two aroylhydrazone derivatives have been reported. Introduction of one hydroxyl group into H_2L^2 , H_3L^1 not only displays a strong interaction with Zn^{2+} but also distinguishes this metal cation from other metal cations, including the strong competitors Cd^{2+} , Mg^{2+} and Ca^{2+} . The increase in emission in the presence of Zn^{2+} is accounted for by the formation of metal-ligand complexes **1** and **2**. An approximately 25-fold Zn^{2+} -selective chelation-enhanced fluorescence response of H_3L^1 is attributed to the strong coordination of Zn^{2+} that would impose rigidity. In our present work, H_3L^1 exhibits a more sensitive and selective binding ability toward the Zn^{2+} ion than H_2L^2 in aqueous ethanol solution, implying that the hydroxyl group substituent structure is superior to the no substituent group for Zn^{2+} binding in this case. The possible reason is the substituent hydroxyl group gives a better chelating ability for Zn^{2+} ion. The different substituting group results in different structures of the complexes. This idea is supported by the structure of $[\text{Zn}(\text{HL}^1)\text{C}_2\text{H}_5\text{OH}]_n$ and $[\text{Zn}_2(\text{HL}^2)_2(\text{CH}_3\text{COO})_2(\text{C}_2\text{H}_5\text{OH})]$.

Acknowledgements

The authors acknowledge the financial support from the NSFC (Grant Nos. 20771048, 20931003, 21001059) and the Funda-

mental Research Funds for the Central Universities (Izujbky-2009-k06).

Notes and references

- B. L. Vallee and K. H. Falchuk, *Physiol. Rev.*, 1993, **73**, 79–118.
- (a) E. Ho and B. N. Ames, *Proc. Natl. Acad. Sci. U. S. A.*, 2002, **99**, 16770–16775; (b) H. Daiyasu, K. Osaka, Y. Ishino and H. Toh, *FEBS Lett.*, 2001, **503**, 1–6.
- A. Q. Troung-Tran, J. Carter, R. E. Ruffin and P. D. Zaleski, *BioMetals*, 2001, **14**, 315–330.
- (a) E. F. Rostan, H. V. DeBuys, D. L. Madey and S. R. Pinnell, *Int. J. Dermatol.*, 2002, **41**, 606–611; (b) Z. Sztányi, C. Nemes and N. Rozlosnik, *Cent Eur. J. Occup. Environ. Med.*, 1998, **4**, 51.
- (a) E. M. Nolan and S. J. Lippard, *Inorg. Chem.*, 2004, **43**, 8310–8317; (b) E. M. Nolan, S. C. Burdette, J. H. Herve, S. A. Hilderbrand and S. J. Lippard, *Inorg. Chem.*, 2004, **43**, 2624–2635; (c) S. Aoki, D. Kagata, M. Shiro, K. Takeda and E. Kimura, *J. Am. Chem. Soc.*, 2004, **126**, 13377–13390; (d) N. C. Lim, J. V. Schuster, M. C. Porto, M. A. Tanudra, L. Yao, H. C. Freake and C. Brückner, *Inorg. Chem.*, 2005, **44**, 2018–2030; (e) R. Parkesh, T. C. Lee and T. Gunnlaugsson, *Org. Biomol. Chem.*, 2007, **5**, 310–317; (f) L. Xue, H. Wang, X. Wang and H. Jiang, *Inorg. Chem.*, 2008, **47**, 4310–4318; (g) N. Williams, W. Gan, J. Reibenspies and R. Hancock, *Inorg. Chem.*, 2009, **48**, 1407–1415.
- (a) G. Dilek and E. U. Akkaya, *Tetrahedron Lett.*, 2000, **41**, 3721–3724; (b) S. Maruyama, K. Kikuchi, T. Hirano, Y. Urano and T. Nagano, *J. Am. Chem. Soc.*, 2002, **124**, 10650–10651; (c) Y. Mikata, M. Wakamatsu, A. Kawamura, N. Yamanaka, S. Yano, A. Odani, K. Morihiro and S. Tamotsu, *Inorg. Chem.*, 2006, **45**, 9262–9268; (d) Y. Mikata, A. Yamanaka, A. Yamashita and S. Yano, *Inorg. Chem.*, 2008, **47**, 7295–7301; (e) X. M. Meng, M. Z. Zhu, L. Liu and Q. X. Guo, *Tetrahedron Lett.*, 2006, **47**, 1559–1562; (f) Y. Zhang, X. F. Guo and X. H. Qiang, *Org. Lett.*, 2008, **10**, 473–476; (g) N. C. Lim, H. C. Freake and C. Brückner, *Chem.–Eur. J.*, 2005, **11**, 38–49; (h) E. Tamanini, K. Flavin, M. Motevalli, S. Piperno, L. A. Gheber, M. H. Todd and M. Watkinson, *Inorg. Chem.*, 2010, **49**, 3789–3800.
- (a) K. Kikuchi, K. Komatsu and T. Nagano, *Curr. Opin. Chem. Biol.*, 2004, **8**, 182–191; (b) P. Jiang and Z. Guo, *Coord. Chem. Rev.*, 2004, **248**, 205–229; (c) R. B. Thompson, *Curr. Opin. Chem. Biol.*, 2005, **9**, 526–532; (d) P. Carol, S. Sreejith and A. Ajayaghosh, *Chem.–Asian J.*, 2007, **2**, 338–348; (e) Z. Dai and J. W. Canary, *New J. Chem.*, 2007, **31**, 1708–1718; (f) S. Mizukami, S. Okada, S. Kimura and K. Kikuchi, *Inorg. Chem.*, 2009, **48**, 7630–7638; (g) C. Bazzicalupi, A. Bencini, S. Biagini, E. Faggi, G. Farruggia, G. Andreani, P. Gratteri, d L. Prodi, A. Spezia and B. Valtancoli, *Dalton Trans.*, 2010, **39**, 7080–7090.
- (a) D. Y. Wu, L. X. Xie, C. L. Zhang, C. Y. Duan, Y. G. Zhao and Z. J. Guo, *Dalton Trans.*, 2006, 3528–3533; (b) N. Singhal, B. Ramanujam, V. Mariappanadar and C. Rao, *Org. Lett.*, 2006, **8**, 3525–3528; (c) F. Zapata, A. Caballero, A. Espinosa, A. Tárraga and P. Molina, *Org. Lett.*, 2007, **9**, 2385–2388.
- S. Ou, Z. Lin, C. Duan, H. Zhang and Z. Bai, *Chem. Commun.*, 2006, 4392–4394.
- (a) P. Roy, K. Dhara, M. Manassero, J. Ratha and P. Banerjee, *Inorg. Chem.*, 2007, **46**, 6405–6412; (b) Z. Wu, Y. Zhang, J. Ma and G. Yang, *Inorg. Chem.*, 2006, **45**, 3140–3142; (c) Y. G. Zhao, B. G. Zhang, C. Y. Duan, Z. H. Lin and Q. J. Meng, *New J. Chem.*, 2006, **30**, 1207–1213; (d) H. GoIrner, S. Khanra, T. Weyhermüller and P. Chaudhuri, *J. Phys. Chem. A*, 2006, **110**, 2587–2594.
- Z. C. Xu, J. Yoon and D. R. Spring, *Chem. Soc. Rev.*, 2010, **39**, 1996–2006.
- G. Q. Yang, F. Morlet-Savary, Z. K. Peng, S. K. Wu and J. P. Fouassier, *Chem. Phys. Lett.*, 1996, **256**, 536–542.
- D. Matoga, J. Szklarzewicz, K. Stadnicka, Shongwe and S. Musa, *Inorg. Chem.*, 2007, **46**, 9042–9044.
- (a) A. Mallick and N. Chahattopadhyay, *Photochem. Photobiol.*, 2005, **81**, 419–424; (b) H. A. Benesi and J. H. Hildebrand, *J. Am. Chem. Soc.*, 1949, **71**, 2703–2707.
- M. Sarkar, S. Banthia and A. Samanta, *Tetrahedron Lett.*, 2006, **47**, 7575–7578.
- P. J. Jiang, L. Z. Chen, J. Lin, Q. Liu, J. Ding, X. Gao and Z. J. Guo, *Chem. Commun.*, 2002, 1424–1425.
- J. S. Wu, W. M. Liu, X. Q. Zhuang, F. Wang, P. F. Wang, S. L. Tao, X. H. Zhang, S. K. Wu and S. T. Lee, *Org. Lett.*, 2007, **9**, 33–36.